GRIFFITH UNIVERSITY

Structure of Streptococcus agalactiae glyceraldehyde-3-phosphate dehydrogenase holoenzyme reveals a novel surface

Author

Ayres, Chapelle A, Schormann, Norbert, Senkovich, Olga, Fry, Alexandra, Banerjee, Surajit, Ulett, Glen C, Chattopadhyay, Debasish

Published

2014

Journal Title

Acta Crystallographica Section F

DOI

10.1107/S2053230X14019517

Downloaded from

http://hdl.handle.net/10072/65419

Griffith Research Online

https://research-repository.griffith.edu.au

CrossMark

electronic reprint

Acta Crystallographica Section F
Structural Biology Communications
ISSN 2053-230X

Structure of *Streptococcus agalactiae* glyceraldehyde-3-phosphate dehydrogenase holoenzyme reveals a novel surface

Chapelle A. Ayres, Norbert Schormann, Olga Senkovich, Alexandra Fry, Surajit Banerjee, Glen C. Ulett and Debasish Chattopadhyay

Acta Cryst. (2014). F**70**, 1333–1339

Copyright © International Union of Crystallography

Author(s) of this paper may load this reprint on their own web site or institutional repository provided that this cover page is retained. Republication of this article or its storage in electronic databases other than as specified above is not permitted without prior permission in writing from the IUCr.

For further information see http://journals.iucr.org/services/authorrights.html

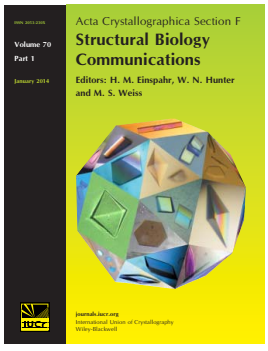

Acta Crystallographica Section F: Structural Biology Communications is a rapid all-electronic journal, which provides a home for short communications on the crystallization and structure of biological macromolecules. Structures determined through structural genomics initiatives or from iterative studies such as those used in the pharmaceutical industry are particularly welcomed. Articles are available online when ready, making publication as fast as possible, and include unlimited free colour illustrations, movies and other enhancements. The editorial process is completely electronic with respect to deposition, submission, refereeing and publication.

Crystallography Journals Online is available from **journals.iucr.org**

Acta Crystallographica Section F
Structural Biology Communications
ISSN 2053-230X

Structure of *Streptococcus agalactiae* glyceraldehyde-3-phosphate dehydrogenase holoenzyme reveals a novel surface

Chapelle A. Ayres,[a]‡ Norbert Schormann,[b]‡ Olga Senkovich,[c] Alexandra Fry,[a] Surajit Banerjee,[d] Glen C. Ulett[e] and Debasish Chattopadhyay[b,c]*

[a]Science and Technology Honors Program, University of Alabama at Birmingham, Birmingham, AL 35294, USA, [b]Center for Biophysical Sciences and Engineering, University of Alabama at Birmingham, Birmingham, AL 35294, USA, [c]Department of Medicine, University of Alabama at Birmingham, Birmingham, AL 35294, USA, [d]Northeastern Collaborative Access Team and Department of Chemistry and Chemical Biology, Cornell University, Argonne, IL 60439, USA, and [e]School of Medical Science and Griffith Health Institute, Griffith University, QLD 4222, Australia

‡ These authors made an equal contribution.

Correspondence e-mail: debasish@uab.edu

Received 28 July 2014
Accepted 28 August 2014

PDB reference: GBS GAPDH, 4qx6

© 2014 International Union of Crystallography
All rights reserved

Glyceraldehyde-3-phosphate dehydrogenase (GAPDH) is a conserved cytosolic enzyme, which plays a key role in glycolysis. GAPDH catalyzes the oxidative phosphorylation of D-glyceraldehyde 3-phosphate using NAD or NADP as a cofactor. In addition, GAPDH localized on the surface of some bacteria is thought to be involved in macromolecular interactions and bacterial pathogenesis. GAPDH on the surface of group B streptococcus (GBS) enhances bacterial virulence and is a potential vaccine candidate. Here, the crystal structure of GBS GAPDH from *Streptococcus agalactiae* in complex with NAD is reported at 2.46 Å resolution. Although the overall structure of GBS GAPDH is very similar to those of other GAPDHs, the crystal structure reveals a significant difference in the area spanning residues 294–307, which appears to be more acidic. The amino-acid sequence of this region of GBS GAPDH is also distinct compared with other GAPDHs. This region therefore may be of interest as an immunogen for vaccine development.

1. Introduction

Glyceraldehyde-3-phosphate dehydrogenase (GAPDH; EC 1.2.1.12) is a highly conserved cytosolic enzyme which plays a central role in the glycolytic pathway for energy metabolism. GAPDH catalyzes the oxidative phosphorylation of D-glyceraldehyde 3-phosphate (D-G3H) to give 1,3-diphosphoglyceric acid and uses NAD or NADP as a cofactor. In the first step of this two-step reaction the active-site cysteine residue of GAPDH attaches covalently to D-G3H and forms a thiohemiacetal intermediate, which transfers a hydride ion to NAD, resulting in the formation of the thioacyl enzyme. In the second step the resulting thioester is phosphorylated through the nucleophilic attack of an inorganic phosphate ion (P_i) on the carbonyl C atom of the thioacyl group, which leads to the formation of 1,3-diphosphoglycerate. In addition to the cytoplasmic form, in recent years surface-localized forms of GAPDH have been identified in a number of microorganisms. These GAPDH forms attach to a variety of macromolecules on target cell surfaces and are shown to be associated with adherence (Jin *et al.*, 2005; Boël *et al.*, 2005), evasion (Terao *et al.*, 2006), adhesion (Maeda *et al.*, 2004), apoptosis (Oliveira *et al.*, 2012) and other alternative functions (Lama *et al.*, 2009), and are thought to be involved in bacterial pathogenesis (Pancholi & Chhatwal, 2003). These proteins are also called anchorless surface proteins because they lack the N-terminal signal sequences required for export and the typical C-terminal hydrophobic tails found in surface-anchored proteins. Since its initial identification in group A streptococcus (GAS; also known as *Streptococcus pyogenes*; Pancholi & Fischetti, 1992) it has been found in other streptococcal species, including *S. agalactiae* (also known as group B streptococcus or GBS; Seifert *et al.*, 2003). An estimated 15–40% of all pregnant women harbor GBS in their vagina or rectum and are clinically classified as GBS positive or GBS colonized. Approximately 40–70% of colonized mothers can pass GBS to babies during childbirth. GBS infection is a leading cause of neonatal sepsis and meningitis even in developed countries (LeDoare & Heath, 2013; Fluegge *et al.*, 2006; Kalliola *et al.*, 1999).

electronic reprint

GAPDH released in the culture supernatant from GBS acts as an immune-modulatory protein facilitating colonization (Madureira *et al.*, 2007). GAPDH localized on the GBS surface has also been shown to enhance bacterial virulence through its interaction with the human plasminogen system (Magalhães *et al.*, 2007). Recently, Oliveira *et al.* (2012) showed that GAPDH released from lysed GBS attaches to the bacterial surface and induces apoptosis in murine macrophages, a process that has been implicated in the pathogenesis of GBS infection (Ulett & Adderson, 2006). Recent data also demonstrated that immunization of mice with rGAPDH induces antibodies that can protect offspring against lethal GBS infections. This suggests that it could be a potential vaccine candidate (Madureira *et al.*, 2011). Together, these data indicate that GBS GAPDH is an important molecule to characterize at the molecular level to gain insight into its function both in terms of disease pathogenesis and its potential as a vaccine candidate against this important human pathogen. The three-dimensional structure of GBS GAPDH may provide insight into the nature and conformation of the surface-exposed epitopes of the protein that may be involved in novel functions. In this communication, we report the crystal structure of *S. agalactiae* GAPDH in complex with its cofactor nicotinamide adenine dinucleotide.

2. Materials and methods

2.1. Protein expression and purification

The coding sequence for *S. agalactiae* GAPDH was amplified from the genomic DNA of the reference GBS strain NEM316 and was subcloned into pET-15b vector (Novagen) into the *Nde*I and *Xho*I sites. The recombinant protein was expressed in *Escherichia coli* BL21(DE3)pLysS Rosetta cells (Invitrogen). The resulting protein (rGAPDH) contains a 20-residue insert (MGSSHHHHHHSSG-**LVPR**GSH) at the N-terminus comprising a hexahistidine tag (underlined) and a thrombin cleavage site (bold). An overnight culture was grown at 310 K in LB medium containing 50 µg ml^{-1} ampicillin and 34 µg ml^{-1} chloramphenicol. The overnight culture was diluted 1:100 in LB medium containing the same composition of antibiotics supplemented with 0.2% glucose and grown at 310 K. When the OD_{595} of the culture reached 0.8–0.9, isopropyl β-D-1-thiogalactopyranoside (IPTG) was added to a final concentration of 0.4 m*M* and the culture was grown for 20 h at 298 K. Cultures were grown with a constant shaking at 225–250 rev min^{-1}. The cell culture was centrifuged at 6700*g* for 15 min at 277 K. Cell pellets were stored at 193 K until further use.

Table 1
Data-collection and refinement statistics for *S. agalactiae* GAPDH (PDB entry 4qx6).

Values in parentheses are for the highest resolution shell.

Wavelength (Å)	0.97918
Space group	$P2_1$
Unit-cell parameters (Å, °)	a = 67.77, b = 107.86, c = 90.93, $\alpha = \gamma$ = 90, β = 106.57
Data-collection statistics	
Resolution limits (Å)	107.86–2.46 (2.59–2.46)
R_{merge}†	0.091 (1.015)
R_{meas}†	0.107 (1.181)
$R_{p.i.m.}$†	0.055 (0.601)
Total No. of observations	170091 (24948)
No. of reflections	45263 (6546)
Mean $I/\sigma(I)$	13.8 (1.3)
$CC_{1/2}$	0.996 (0.567)
Completeness (%)	99.3 (99.0)
Multiplicity	3.8 (3.8)
Refinement statistics	
Resolution range (Å)	64.96–2.46 (2.52–2.46)
No. of unique reflections	45232 (3296)
R_{cryst}‡ (%)	20.4 (34.5)
R_{free}‡ (%)	23.8 (35.2)
No. of protein residues	1345
No. of NAD molecules	4
No. of EDO molecules	2
No. of water molecules	126
Wilson B factor (Å^2)	48.4
Average B factors (Å^2)	
Overall	57.4
Protein	57.8
NAD	46.0
EDO	62.0
Water	42.1
Coordinate error (maximum likelihood)	0.26
Correlation coefficient, $F_o - F_c$	0.95
Correlation coefficient, $F_o - F_c$ free	0.93
Overall map CC (F_c, $2mF_o - DF_c$)	0.76§
Ramachandran allowed (%)	99.8
Ramachandran disallowed (%)	0.2
MolProbity clash score	3.4 [100th percentile]
MolProbity score	1.5 [99th percentile]

† R_{meas} and $R_{p.i.m.}$ were calculated with *SCALA* (Evans, 2006) in the *CCP*4 program suite (Winn *et al.*, 2011) using unmerged and unscaled data preprocessed by *XDS* (Kabsch, 2010*a*,*b*). R_{meas} is a merging R factor independent of data redundancy, while $R_{p.i.m.}$ provides the precision of the averaged measurement, which improves with higher multiplicity (Weiss, 2001). ‡ The data included in the R_{free} set (5%) were excluded from refinement. § The value based on map calculation in *PHENIX* (Adams *et al.*, 2010).

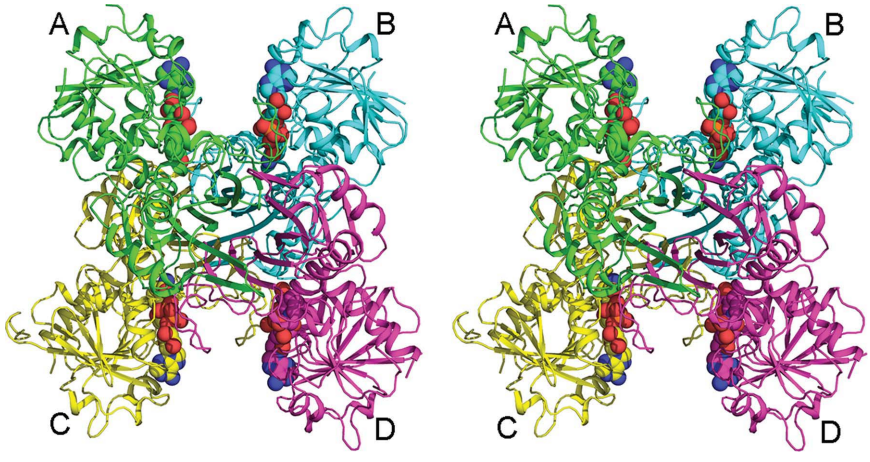

Figure 1
Tetrameric assembly of GBS GAPDH. The stereo diagram figure shows the tetrameric assembly (noncrystallographic 222 symmetry) of GBS GAPDH in the asymmetric unit (biological assembly). Individual protein subunits are labeled and represented as ribbon drawings colored by chain (*A*, green; *B*, cyan; *C*, yellow; *D*, magenta). NAD molecules are shown as spheres (color code: C, colored by chain as for protein subunits; O, red; N, blue; P, orange).

electronic reprint

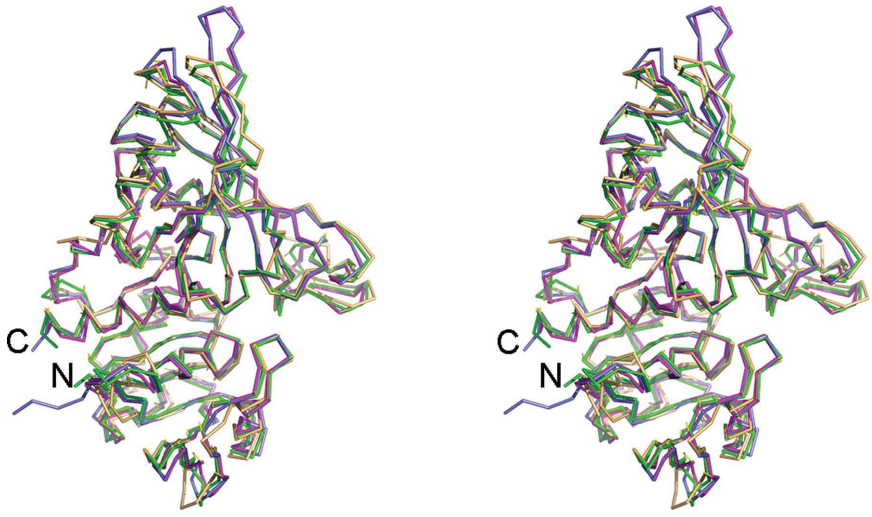

Figure 2
Superimposition of GAPDHs from different species. The stereo drawing shows the superimposition of one subunit of GBS (PDB entry 4qx6), *S. aureus* (PDB entry 3lvf), *C. parvum* (PDB entry 1vsv) and human (PDB entry 3gpd) GAPDH. The C$^{\alpha}$ traces of GAPDH subunits are shown (color code: 4qx6, magenta; 3lvf, blue; 1vsv, green; 3gpd, wheat).

Recombinant protein was purified at 277 K by immobilized metal (cobalt) affinity chromatography and size-exclusion chromatography. Frozen bacterial cell pellets from 2 l cell cultures were suspended in 45 ml lysis buffer composed of 25 m*M* HEPES pH 7.35, 0.1 *M* NaCl, 5 m*M* β-mercaptoethanol, 0.2 m*M* phenylmethylsulfonyl fluoride, 5 m*M* benzamidine hydrochloride. After two freeze–thaw cycles, the lysate was incubated for 30 min at 277 K with 0.5 mg ml^{-1} DNAse I followed by centrifugation at 46 000*g* for 20 min at 277 K. The supernatant was loaded onto a TALON column (Clontech Laboratories) equilibrated with lysis buffer. The column was then washed with wash buffer (lysis buffer with NaCl concentration increased to 0.3 *M* containing 25 m*M* imidazole). Bound protein was eluted using a linear gradient of imidazole (25–300 m*M*) in 20 column volumes of lysis buffer. Eluted fractions were analyzed by SDS–PAGE). Fractions containing homogeneous protein samples were pooled and concentrated ∼30-fold using a 30 kDa cutoff (YM30 membrane) in an Amicon ultracentrifugal unit (EMD Millipore Chemicals). The concentrated protein was applied onto a Superdex 200 HR 26/60 column (GE Healthcare Life Sciences) equilibrated with two column volumes of 25 m*M* HEPES buffer pH 7.35, 0.1 *M* NaCl, 5 m*M* β-mercaptoethanol. Protein samples eluted in the peak fractions were analyzed by SDS–PAGE and the most homogeneous fractions were

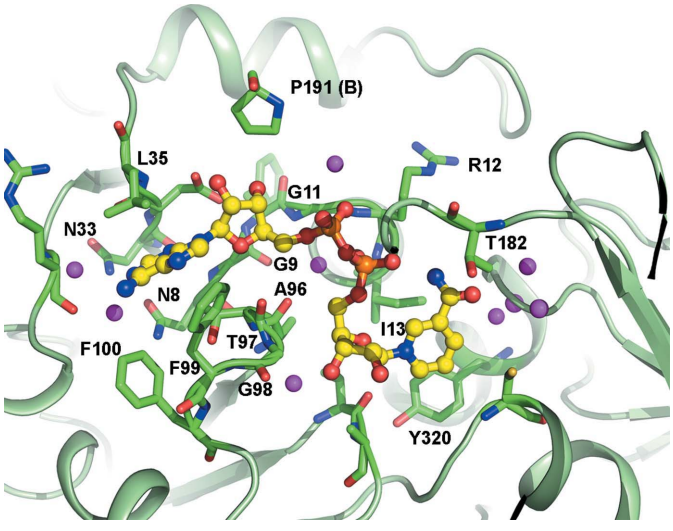

Figure 3
Close-up view of the active site in GBS GAPDH. The protein is represented as a ribbon model in green. Protein residues within 4 Å of the NAD molecule are shown as stick models (color code: C, green; O, red; N, blue) and are labeled. The NAD molecule in the center is displayed as a ball-and-stick representation (color code: C, yellow; O, red; N, blue; P, orange). Water molecules are shown as purple spheres.

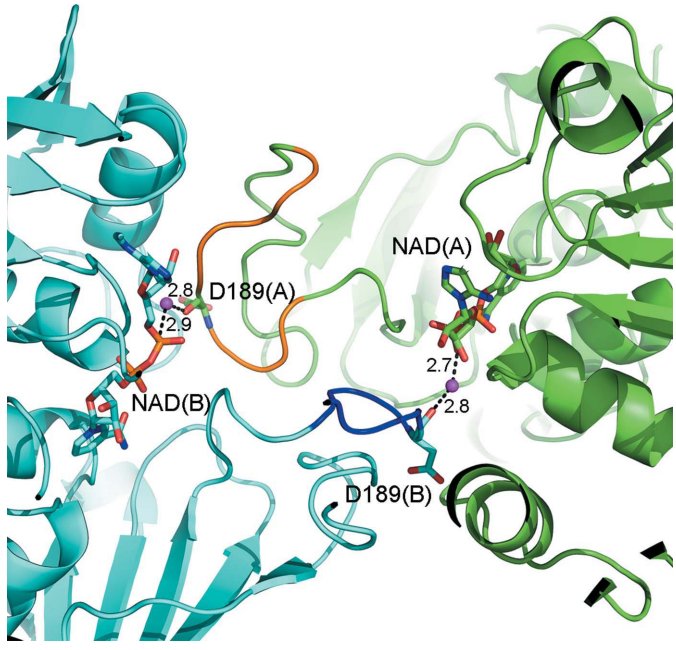

Figure 4
S-loop in GBS GAPDH. The figure shows interactions of protein residue Asp189 (backbone O atom) in subunits *A* and *B* through a water molecule with the NAD molecule of the neighboring protein subunit. The two protein subunits are shown as ribbon models colored by chain (*A*, green; *B*, cyan). Residue Asp189 and NAD molecules in subunits *A* and *B* are represented as stick models (color code: C, same color as corresponding protein subunit; O, red; N, blue; P, orange). The water molecules are shown as purple spheres. Protein subunits (*A* and *B*) and residue Asp189 (in subunits *A* and *B*) are labeled. Hydrogen-bonding distances are shown as dashed black lines.

electronic reprint

pooled and concentrated to a final concentration of 8.9 mg ml^{-1}. No attempt was made to cleave the histidine tag from GBS GAPDH. Upon size-exclusion chromatography, GBS GAPDH eluted at a volume (∼180 ml) expected for a tetrameric protein. Protein aliquots were flash-frozen and stored at 193 K until further use. The final yield after gel filtration was ∼18 mg in total (from 2 l cell culture).

2.2. Crystallization, intensity data collection and processing

Concentrated rGAPDH was subjected to crystallization screening at room temperature using a number of commercial crystallization kits. Crystals, which were mostly needle-shaped, were obtained in several crystallization solutions. Crystals suitable for data collection were grown using the microseeding technique in 26–36% polyethylene glycol (PEG) 4000, 0.1 *M* MES buffer pH 6.5. Needle-shaped crystals were washed thoroughly by transferring them into 100 µl reservoir solution on a depression plate and were crushed in fresh reservoir solution to make a seed stock. The seed stock was diluted 1:10, 1:100 and 1:1000 in reservoir solution. Hanging drops were prepared by mixing 2 µl protein plus cofactor mixture, 0.5 µl water and 0.5 µl reservoir solution containing seed suspension in a cover slip, which was then sealed over a 500 µl reservoir and incubated at 295 K. The reservoir solution for growing the crystal used for structure determination consisted of 28% PEG 4000, 0.1 *M* MES buffer pH 6.5. Recently, crystallization of *S. agalactiae* in an isomorphous crystal form has been reported (Nagarajan & Ponnuraj, 2014). These crystals were also grown from PEG 4000 and PEG 3350 at 287 K, but the crystallization buffer was composed of 0.1 *M* Tris–HCl pH 8.0–9.0.

For data collection, a crystal (0.3 × 0.2 × 0.15 mm) was transferred serially into reservoir solutions supplemented with 15, 18 and 20%(*v*/*v*) glycerol and then flash-cooled in liquid nitrogen. Data were collected using a PILATUS 6M detector on NE-CAT beamline 24-ID-C at the Advanced Photon Source (APS). A total of 180° of oscillation data (1° per frame) were collected. Data were processed with *XDS* (Kabsch, 2010*a*,*b*) and *SCALA* (Evans, 2006) in the *CCP*4 suite (Winn *et al.*, 2011) as part of the *RAPD* data-collection strategy at NE-CAT (https://rapd.nec.aps.anl.gov/rapd).

2.3. Structure determination and refinement

Examination of GAPDH sequence alignments using the *LALIGN* server (http://www.ch.embnet.org/software/LALIGN_form.html) suggested that GBS GAPDH showed the best local alignment (68.8% identity) with the primary sequence of *S. aureus* MRSA strain 252 GAPDH (http://www.uniprot.org/uniprot/Q6GIL8). We therefore prepared a search model using the tetrameric crystal structure of *S. aureus* GAPDH (PDB entry 3lvf; Mukherjee *et al.*, 2010) by removing the coordinates for the cofactor and water molecules. The crystal structure was solved by molecular replacement using *PHENIX* (Adams *et al.*, 2010), which was used for initial model building and refinement. After initial refinement, one NAD molecule

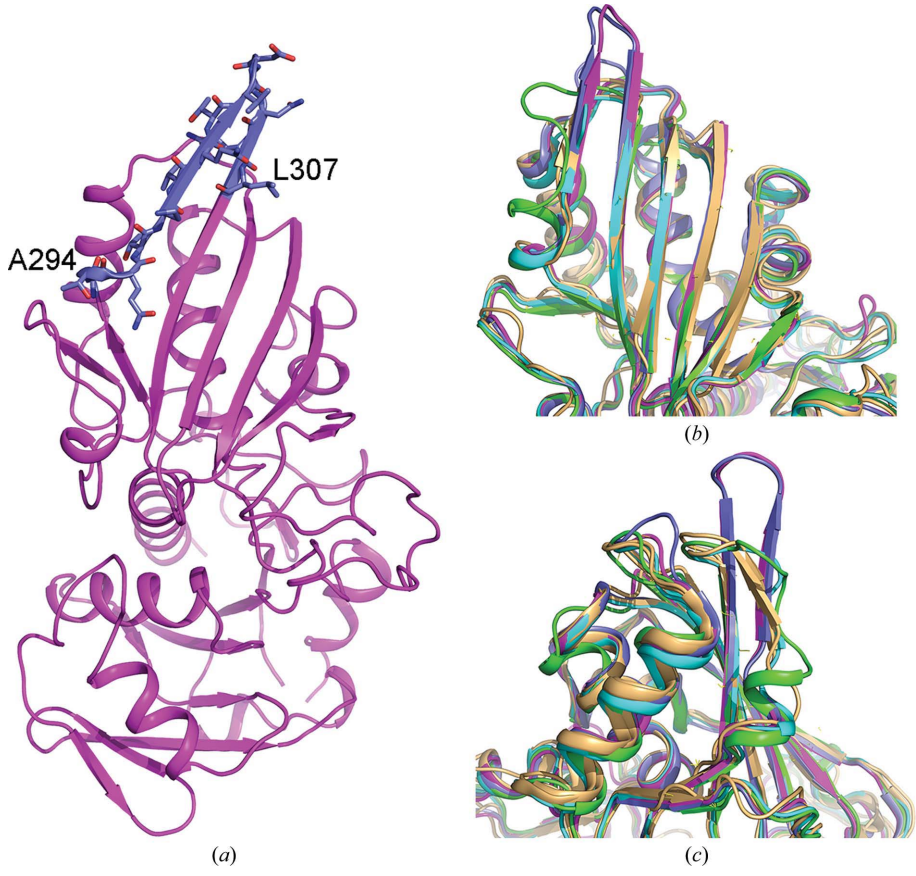

Figure 5
Structural difference in GBS GAPDH. The figure shows a comparison of the diverse region 294–307 as observed in GBS (PDB entry 4qx6) and *S. aureus* (PDB entry 3lvf) GAPDH with *C. parvum* (PDB entry 1vsv) and human (PDB entry 3gpd) GAPDH. (*a*) A cartoon drawing of subunit *A* of GBS GAPDH is shown in magenta. The segment of the secondary structure spanning residues 294–307 is colored blue and the amino-acid residues in this region are shown as stick models. (*b*, *c*) Two different views showing superimposition of GAPDH subunits from GBS, *S. aureus*, *C. parvum* and human in two different views are shown to emphasize the differences in the region highlighted above (color code: GBS GAPDH, magenta; 3lvf, blue; 1vsv, green; 3gpd, wheat).

electronic reprint

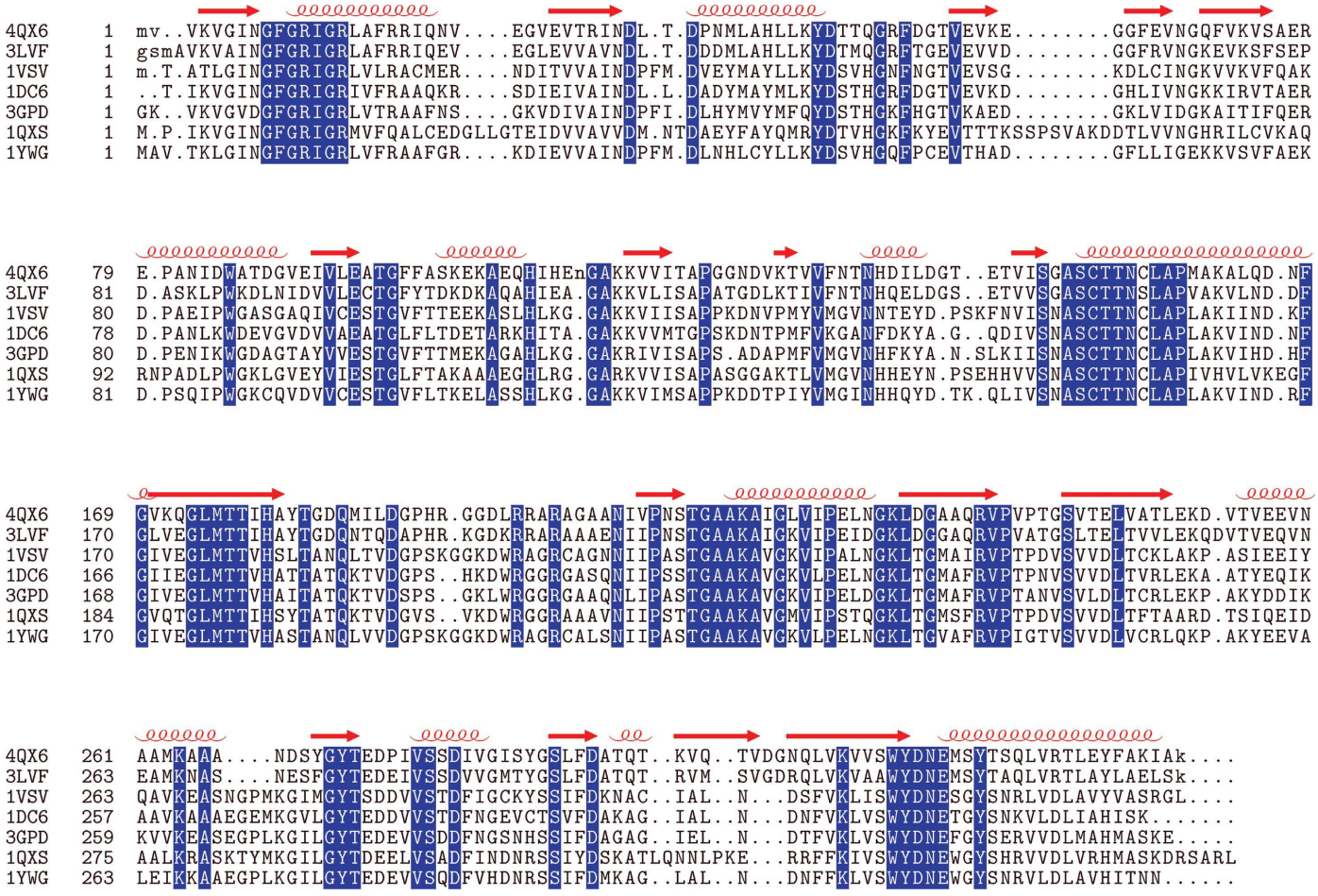

Figure 6
Structure-based sequence alignment of GAPDHs from different species. The figure shows a structure-based sequence alignment of GAPDHs from different species (GBS GAPDH, PDB entry 4qx6; *S. aureus* GAPDH, 3lvf; *C. parvum* GAPDH, 1vsv; *E. coli* GAPDH, 1dc6; human GAPDH, 3gpd; *T. cruzi* GAPDH, 1qxs; *P. falciparum* GAPDH, 1ywg). The secondary-structure annotation at the top is based on GBS GAPDH (β-strands, red arrows; α-helices, red coils). Conserved residues are highlighted in blue.

could be unambiguously placed in the electron density in each of the four GAPDH molecules. After refinement of protein residues and NAD, water molecules were modeled into a difference electron-density map (3σ contour level) using *Coot* (Emsley & Cowtan, 2004). Final rounds of refinement and model building were performed using *REFMAC*5 (Murshudov *et al.*, 2011) and *Coot*. Data-collection and refinement statistics are listed in Table 1. The final atomic coordinates and structure factors for GBS GAPDH in complex with NAD have been deposited in the PDB as entry 4qx6. All figures were produced with *PyMOL* (DeLano, 2002).

3. Results and discussion

Analysis of the refined structure of GBS GAPDH using *MolProbity* (Chen *et al.*, 2010) indicates that the quality of the model is excellent. A total of 99.8% of the residues in the final model are in the allowed regions of the Ramachandran plot. All three residues in the disallowed region of Ramachandran plot (His111 in chain *A*, Glu112 in chain *B* and Asp127 in chain *D*) are located in solvent-exposed flexible areas of the protein structure, and electron density for these residues is poor.

The asymmetric unit of the crystal structure contains four monomers, *A*, *B*, *C* and *D*, related by noncrystallographic 222 symmetry (Fig. 1). The r.m.s. deviation for pairwise alignment of the monomeric units is less than 0.2 Å. GAPDHs from various organisms maintain a highly conserved structural fold (Seidler, 2012). As expected, the overall structure of the GBS GAPDH monomer is very similar to other GAPDHs (Fig. 2). The r.m.s. deviations for pairwise alignment of a single chain of GBS GAPDH with one chain of *S. aureus* GAPDH and *Cryptosporidum parvum* GAPDH is 0.62 Å (331 aligned C^{α} atoms) and 1.05 Å (327 aligned C^{α} atoms), respectively. Structures of GAPDHs from many organisms have been discussed extensively. We will therefore compare only important structural features of the GBS protein with other GAPDHs.

We crystallized GBS GAPDH in the presence of 2 m*M* NAD. Each subunit in the tetramer contains a bound NAD. As shown in Supplementary Fig. S1[1], the electron density for NAD in each subunit was good except for a portion of the nicotinamide ring. The average *B* factor for the NAD molecules in the *A*, *B*, *C* and *D* subunits is in the range 39.91–51.44 Å^2, while that for all protein residues is 57.8 Å^2. NAD molecules are in an extended conformation (Fig. 3) and are bound by residues from different areas of the protein (Supplementary Table S1). The residues lining the NAD-binding pocket and those directly involved in binding to NAD are highly conserved in the GAPDH sequences from various species.

Binding of the cofactor to GAPDH induces an ordering of a loop designated the S-loop. In the structure of *C. parvum* GAPDH in the

[1] Supporting information has been deposited in the IUCr electronic archive (Reference: EN5556).

electronic reprint

NAD-bound form (PDB entry 1vsv) we noted ordering of the entire S-loop, which was disordered in all subunits of the apo form (PDB entry 1vsu; Cook *et al.*, 2009). In the GBS GAPDH structure the equivalent area (residues 186–194) is well ordered and the residues in this area have some of the lowest *B* factors in the molecules. As in *C. parvum* GAPDH, the S-loop of each subunit makes no contact with the NAD bound to the same subunit but interacts with the cofactor bound to an adjacent subunit through a water molecule; the main-chain O atom of Asp189 in each subunit forms a hydrogen bond to a water molecule, which also forms a hydrogen bond to the pyrophosphate O atom of NAD of the neighboring subunit (Fig. 4).

In some GAPDH structures the active-site cysteine (Cys152 in GBS) is found in multiple conformations in the absence of cofactor (Jenkins & Tanner, 2006). Moreover, NAD binding is associated with the movement of a conserved histidine residue (His179) that results in an altered distance between its NE atom and the S atom of the cysteine residue. In the present structure, the residues immediately preceding the S-loop including His179 are all well ordered, and

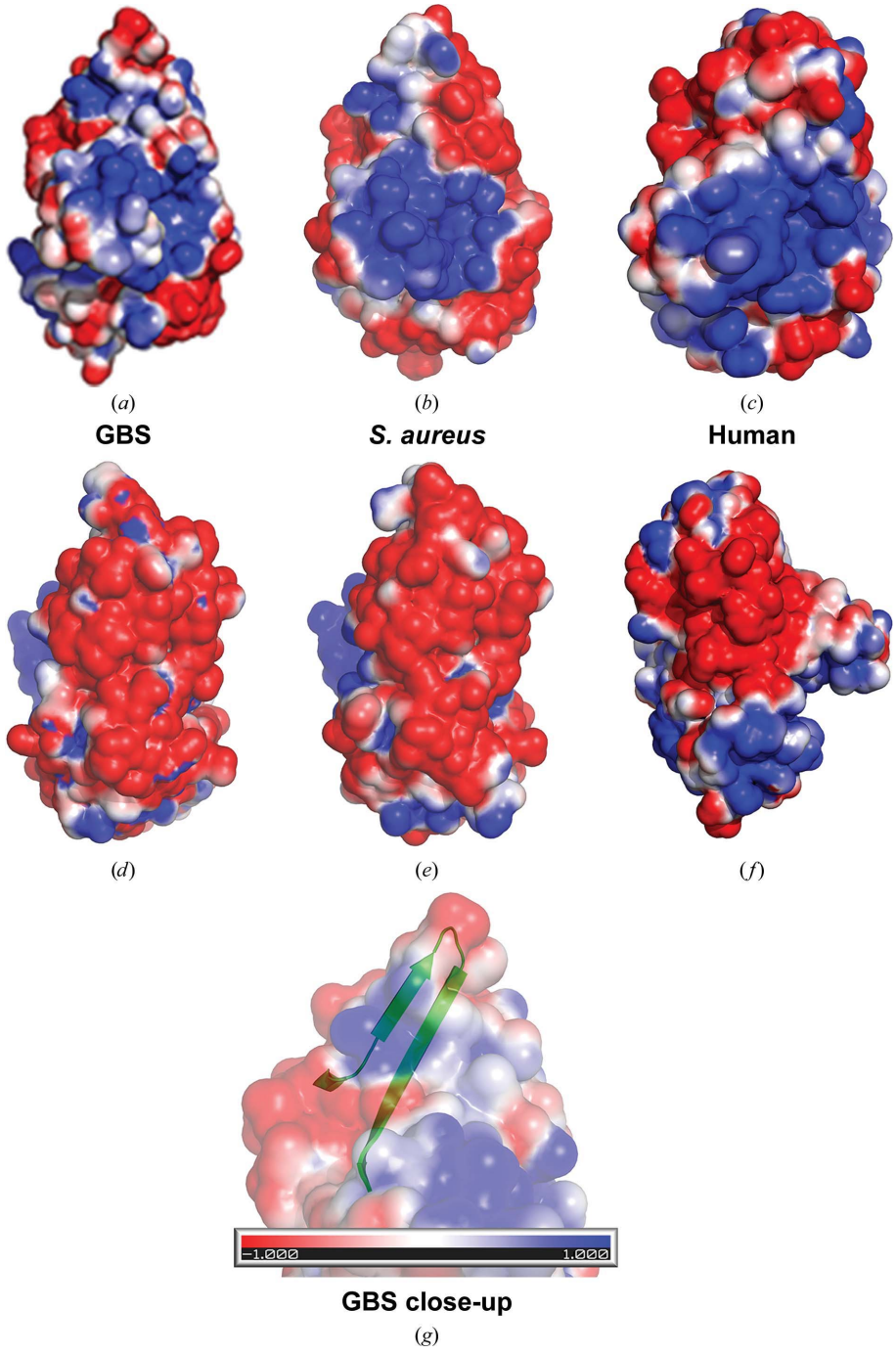

Figure 7
Solvent-accessible surface contoured by electrostatic potential for GBS, *S. aureus* and human GAPDH. Two different views of the solvent-accessible surface of GAPDH with the overlaid electrostatic potential (contoured at $-1\ k_BT/e$ to $+1\ k_BT/e$) are shown. (*a*, *d*) GBS, (*b*, *e*) *S. aureus*, (*c*, *f*) human. (*g*) A close-up view of a portion of GBS GAPDH shown in (*a*). The region of the protein secondary structure (residue range 294–314) is highlighted in green. The orientation of the molecule in (*a*) is similar to that in Figs. 5(*a*) and 5(*b*). The electrostatic potential was calculated using *DelPhi* (Rocchia *et al.*, 2001) and plotted using the *APBS* plugin in *PyMOL* (DeLano, 2002).

electronic reprint

Cys152 in each subunit displays only one conformation. In all subunits the distance between the S atom of Cys152 and the NE atom of His179 is 3.2 Å, suggesting that all subunits of GBS GAPDH are in a similar conformational state (Supplementary Fig. S2).

Three-dimensional structure-based alignment of GAPDHs from various species revealed that the C-terminal β-strands of the GBS and *S. aureus* GAPDHs are considerably longer than in other species (Fig. 5). The corresponding region also represents the area with the most diverse sequence in GAPDHs. The last β-strand of GBS GAPDH (residues 305–314) is connected by a short loop (303–304) to a short antiparallel β-strand (residues 298–302). In the sequence of GBS GAPDH no residue in the range 298–307 is identical to any residue in the equivalent positions of *T. cruzi*, *C. parvum*, *Plasmodium falciparum*, human and *E. coli* GAPDH (Fig. 6). A number of residues immediately upstream of this sequence are also different in human and protozoan GAPDHs. Only two amino-acid residues in this range are identical between the GAPDHs of GBS and *S. aureus*. Visualization of the solvent-accessible surface demonstrated a remarkable difference in the electrostatic potential in this portion of GBS GAPDH. In particular, the loop connecting the two β-strands appears to be more acidic in GBS GAPDH even in comparison to *S. aureus* GAPDH (Fig. 7). Considering the difference in amino-acid sequence and the conformation of this site compared with human GAPDH, this region may be of interest for examination as a potential immunogen for a vaccine candidate. Peptides spanning this area of GBS GAPDH may be able to elicit specific antibody responses. Moreover, this may represent a possible site for the interaction of GBS GAPDH with other macromolecules. Therefore, antibodies targeting this unique site may block the interactions of GADPH with cellular macromolecules and may have additional protective benefits.

The work is based upon research conducted at the Advanced Photon Source on the Northeastern Collaborative Access Team beamlines, which are supported by a grant from the National Institute of General Medical Sciences (P41 GM103403) from the National Institutes of Health. Use of the Advanced Photon Source, an Office of Science User Facility operated for the US Department of Energy (DOE) Office of Science by Argonne National Laboratory, was supported by the US DOE under Contract No. DE-AC02-06CH11357. GCU is supported by an Australian Research Council (ARC) Future Fellowship (FT110101048).

References

Adams, P. D. *et al.* (2010). *Acta Cryst.* D**66**, 213–221.
Boël, G., Jin, H. & Pancholi, V. (2005). *Infect. Immun.* **73**, 6237–6248.
Chen, V. B., Arendall, W. B., Headd, J. J., Keedy, D. A., Immormino, R. M., Kapral, G. J., Murray, L. W., Richardson, J. S. & Richardson, D. C. (2010). *Acta Cryst.* D**66**, 12–21.
Cook, W. J., Senkovich, O. & Chattopadhyay, D. (2009). *BMC Struct. Biol.* **9**, 9.
DeLano, W. L. (2002). *PyMOL*. http://www.pymol.org.
Emsley, P. & Cowtan, K. (2004). *Acta Cryst.* D**60**, 2126–2132.
Evans, P. (2006). *Acta Cryst.* D**62**, 72–82.
Fluegge, K., Siedler, A., Heinrich, B., Schulte-Moenting, J., Moennig, M. J., Bartels, D. B., Dammann, O., von Kries, R. & Berner, R. (2006). *Pediatrics*, **117**, e1139–e1145.
Jenkins, J. L. & Tanner, J. J. (2006). *Acta Cryst.* D**62**, 290–301.
Jin, H., Song, Y. P., Boel, G., Kochar, J. & Pancholi, V. (2005). *J. Mol. Biol.* **350**, 27–41.
Kabsch, W. (2010*a*). *Acta Cryst.* D**66**, 125–132.
Kabsch, W. (2010*b*). *Acta Cryst.* D**66**, 133–144.
Kalliola, S., Vuopio-Varkila, J., Takala, A. K. & Eskola, J. (1999). *Pediatr. Infect. Dis. J.* **18**, 806–810.
Lama, A., Kucknoor, A., Mundodi, V. & Alderete, J. F. (2009). *Infect. Immun.* **77**, 2703–2711.
LeDoare, K. & Heath, P. T. (2013). *Vaccine*, **31**, D7–D12.
Madureira, P., Andrade, E. B., Gama, B., Oliveira, L., Moreira, S., Ribeiro, A., Correia-Neves, M., Trieu-Cuot, P., Vilanova, M. & Ferreira, P. (2011). *PLoS Pathog.* **7**, e1002363.
Madureira, P., Baptista, M., Vieira, M., Magalhães, V., Camelo, A., Oliveira, L., Ribeiro, A., Tavares, D., Trieu-Cuot, P., Vilanova, M. & Ferreira, P. (2007). *J. Immunol.* **178**, 1379–1387.
Maeda, K., Nagata, H., Kuboniwa, M., Kataoka, K., Nishida, N., Tanaka, M. & Shizukuishi, S. (2004). *Infect. Immun.* **72**, 5475–5477.
Magalhães, V., Veiga-Malta, I., Almeida, M. R., Baptista, M., Ribeiro, A., Trieu-Cuot, P. & Ferreira, P. (2007). *Microbes Infect.* **9**, 1276–1284.
Mukherjee, S., Dutta, D., Saha, B. & Das, A. K. (2010). *J. Mol. Biol.* **401**, 949–968.
Murshudov, G. N., Skubák, P., Lebedev, A. A., Pannu, N. S., Steiner, R. A., Nicholls, R. A., Winn, M. D., Long, F. & Vagin, A. A. (2011). *Acta Cryst.* D**67**, 355–367.
Nagarajan, R. & Ponnuraj, K. (2014). *Acta Cryst.* F**70**, 938–941.
Oliveira, L., Madureira, P., Andrade, E. B., Bouaboud, A., Morello, E., Ferreira, P., Poyart, C., Trieu-Cuot, P. & Dramsi, S. (2012). *PLoS One*, **7**, e29963.
Pancholi, V. & Chhatwal, G. S. (2003). *Int. J. Med. Microbiol.* **293**, 391–401.
Pancholi, V. & Fischetti, V. A. (1992). *J. Exp. Med.* **176**, 415–426.
Rocchia, W., Alexov, E. & Honig, B. (2001). *J. Phys. Chem. B*, **105**, 6507–6514.
Seidler, N. W. (2012). *GAPDH: Biological Properties and Diversity*. Dordrecht: Springer.
Seifert, K. N., McArthur, W. P., Bleiweis, A. S. & Brady, L. J. (2003). *Can. J. Microbiol.* **49**, 350–356.
Terao, Y., Yamaguchi, M., Hamada, S. & Kawabata, S. (2006). *J. Biol. Chem.* **281**, 14215–14223.
Ulett, G. C. & Adderson, E. E. (2006). *Curr. Immunol. Rev.* **2**, 119–141.
Weiss, M. S. (2001). *J. Appl. Cryst.* **34**, 130–135.
Winn, M. D. *et al.* (2011). *Acta Cryst.* D**67**, 235–242.

electronic reprint